

Supporting Information

for *Adv. Optical Mater.*, DOI: 10.1002/adom.202203139

Bright Lanthanide^{III} Triboluminescence despite Low
Photoluminescence, and Dual Triboluminescence and
Mechano-Responsive Photoluminescence

Yuichi Hirai, Stann Van Baaren, Takahito Ohmura,
Takayuki Nakanishi, Takashi Takeda, Yuichi Kitagawa,
Yasuchika Hasegawa, Rémi Métivier, and Clémence
Allain*

Supporting
©Wiley-VCH
69451 Weinheim, Germany

Information
2021

Bright lanthanide^{III} triboluminescence despite low photoluminescence, and dual triboluminescence and mechano-responsive photoluminescence

Yuichi Hirai,^{*,[a]} Stann Van Baaren,^[b] Takahito Ohmura,^[c] Takayuki Nakanishi,^[a] Takashi Takeda,^[a] Yuichi Kitagawa,^[d,e] Yasuchika Hasegawa,^[d,e] Rémi Métivier,^[b] Clémence Allain^[b]

Abstract: In pursuit of a new family of mechanically responsive luminescent materials, we aimed to differentiate triboluminescence (TL) from photoluminescence (PL). A β -diketonate ligand with *tert*-butyl groups (2,2,6,6-tetramethylheptane-3,5-dionate: tmh) was selected to quench Eu^{III}-centered PL via ligand-to-metal charge transfer, whereas tmh provided efficient photosensitization of Tb^{III} ions. Bright TL was observed from the Eu^{III} and Tb^{III} homodinuclear complexes despite the fact that their PL quantum yields differed by a factor of >50. Nanomechanical tests revealed the ductility of the crystals, suggesting they are ideal for accumulating deformation energy before breakage. Furthermore, a TL/PL color difference was observed for a Tb^{III}/Eu^{III} heterodinuclear complex, and grinding resulted in mechanochromic luminescence (MCL); this is the first example of a dual TL- and MCL-active lanthanide^{III} coordination compound. The photophysical properties before, during, and after grinding were investigated and correlated with powder and single-crystal crystallographic data.

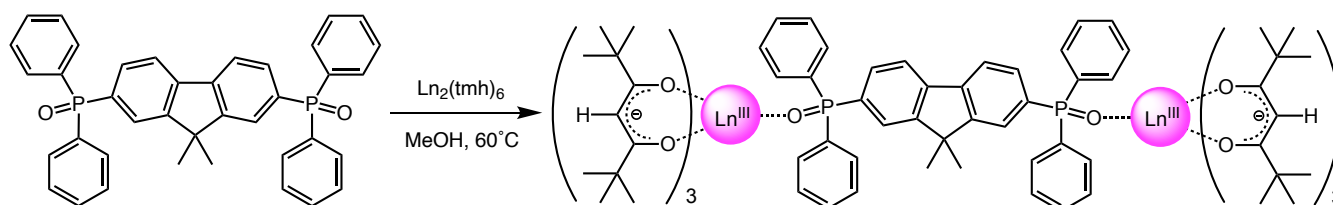
DOI:

SUPPORTING INFORMATION

Experimental Procedures

Materials and methods

Europium chloride hexahydrate (99.9%), terbium chloride hexahydrate (99.9%), 1.6 M *n*-butyllithium solution, and hydrogen peroxide solution were purchased from Sigma Aldrich Co. LLC. 2,7-Dibromo-9,9-dimethylfluorene, dipivaloylmethane and chlorodiphenylphosphine were obtained from TCI Europe N.V. All other chemicals and solvents were reagent grade and were used without further purification. Elemental analyses were performed by a CHN analyzer CE440 (Exeter Analytical, Inc). Mass spectrometry was performed by a JMS-T100LP (JEOL Ltd.).



Scheme S1. Synthetic scheme of dinuclear Ln^{III} complexes ($\text{Ln} = \text{Eu}, \text{Tb}, \text{Gd}$ or Eu/Tb mixture).

Preparation of dinuclear Ln^{III} complexes $\text{Ln}_2(\text{tmh})_6(\text{dpdp})$ ($\text{Ln}_2 = \text{Eu}_2, \text{Tb}_2, \text{Gd}_2$, or Eu/Tb mixture)

2,7-bis(diphenylphosphoryl)-9,9-dimethylfluorene (dpdp, reference 13 in main text) and the precursor complexes $(\text{Ln}(\text{tmh})_3(\text{MeOH}))^{[28]}$ were synthesized according to the literature methods. $\text{Ln}(\text{tmh})_3(\text{MeOH})$ (0.70 mmol) and dpdp (0.21 g, 0.35 mmol) were dissolved in methanol (35 mL), and the mixture was stirred for 6 h at 60 °C. The reaction mixture was concentrated and filtered, then re-dissolved in methanol for recrystallization. The obtained crystals were collected and washed with methanol.

$\text{Eu}_2(\text{tmh})_6(\text{dpdp})$: Yield 0.30 g (43%). ESI-Mass (m/z): calcd for $\text{C}_{94}\text{H}_{127}\text{Eu}_2\text{O}_{12}\text{P}_2$ [$\text{Eu}_2(\text{tmh})_5(\text{dpdp})$] $^+$: 1815.7, found, 1816.7. Anal. Calcd for $\text{C}_{105}\text{H}_{146}\text{Eu}_2\text{O}_{14}\text{P}_2$: C 63.11, H 7.37; found: C 62.59, H 7.06.

$\text{Tb}_2(\text{tmh})_6(\text{dpdp})$: Yield 0.51 g (72%). ESI-Mass (m/z): calcd for $\text{C}_{94}\text{H}_{127}\text{O}_{12}\text{P}_2\text{Tb}_2$ [$\text{Tb}_2(\text{tmh})_5(\text{dpdp})$] $^+$: 1827.7, found, 1828.7. Anal. Calcd for $\text{C}_{105}\text{H}_{146}\text{O}_{14}\text{P}_2\text{Tb}_2$: C 62.68, H 7.31; found: C 62.47, H 7.37.

$\text{Gd}_2(\text{tmh})_6(\text{dpdp})$: Yield 0.49 g (69%). ESI-Mass (m/z): calcd for $\text{C}_{94}\text{H}_{127}\text{Gd}_2\text{O}_{12}\text{P}_2$ [$\text{Gd}_2(\text{tmh})_5(\text{dpdp})$] $^+$: 1825.7, found, 1825.8. Anal. Calcd for $\text{C}_{105}\text{H}_{146}\text{Gd}_2\text{O}_{14}\text{P}_2$: C 62.78, H 7.33; found: C 62.52, H 7.37.

$\text{EuTb}(\text{tmh})_6(\text{dpdp})$: Yield 0.33 g (47%). ESI-Mass (m/z): calcd for $\text{C}_{94}\text{H}_{127}\text{EuO}_{12}\text{P}_2\text{Tb}$ [$\text{EuTb}(\text{tmh})_5(\text{dpdp})$] $^+$: 1821.7, found, 1821.7. Anal. Calcd for $\text{C}_{105}\text{H}_{146}\text{EuO}_{14}\text{P}_2\text{Tb}$: C 62.90, H 7.34; found: C 62.58, H 7.33.

Single-crystal X-ray analysis

Single crystals of $\text{Eu}_2(\text{tmh})_6(\text{dpdp})$, $\text{Tb}_2(\text{tmh})_6(\text{dpdp})$, $\text{Gd}_2(\text{tmh})_6(\text{dpdp})$, and $\text{EuTb}(\text{tmh})_6(\text{dpdp})$ were prepared by slow evaporation of methanol solutions. A colorless block-shaped single crystal was mounted on a MiTiGen micromesh using LV CryoOilTM. The measurements were performed on a Rigaku Synergy Custom system with a Hybrid Pixel Array Detector HyPix-Arc 150 using graphite monochromated Mo-K α radiation. Correction for decay and Lorentz-polarization effects were made using empirical absorption correction, solved by direct methods, and expanded using Fourier techniques. Non-hydrogen atoms were refined anisotropically. Hydrogen atoms were refined using the riding model. All calculations were performed using the Rigaku CrysAlis(Pro) crystallographic software package. CIF data was confirmed by using the checkCIF/PLATON service. CCDC data (2219723: $\text{Eu}_2(\text{tmh})_6(\text{dpdp})$, 2219722: $\text{Tb}_2(\text{tmh})_6(\text{dpdp})$, 2219720: $\text{EuTb}(\text{tmh})_6(\text{dpdp})$, 2219721: $\text{Gd}_2(\text{tmh})_6(\text{dpdp})$) with supplementary crystallographic information for this paper are available free of charge from The Cambridge Crystallographic Data Centre via www.ccdc.cam.ac.uk/data_request/cif.

Table S1. Crystallographic information of $\text{Ln}_2(\text{tmh})_6(\text{dpdp})$ ($\text{Ln}_2 = \text{Eu}_2, \text{Tb}_2, \text{Gd}_2$, or EuTb).

Compound	$\text{Eu}_2(\text{tmh})_6(\text{dpdp})$	$\text{Tb}_2(\text{tmh})_6(\text{dpdp})$	$\text{EuTb}(\text{tmh})_6(\text{dpdp})$	$\text{Gd}_2(\text{tmh})_6(\text{dpdp})$
Formula	$\text{C}_{105}\text{H}_{146}\text{Eu}_2\text{O}_{14}\text{P}_2$	$\text{C}_{105}\text{H}_{146}\text{O}_{14}\text{P}_2\text{Tb}_2$	$\text{C}_{105}\text{H}_{146}\text{Eu}_1\text{O}_{14}\text{P}_2\text{Tb}_1$	$\text{C}_{105}\text{H}_{146}\text{Gd}_2\text{O}_{14}\text{P}_2$
Dcalc./g cm ⁻³	1.267	1.278	1.277	1.271
m/mm ⁻¹	1.274	1.429	1.356	1.340
Formula Weight	1998.07	2011.99	2005.02	2008.65
Colour	colourless	colourless	colourless	colourless
Shape	sphere	sphere	sphere	sphere
Size/mm ³	0.09×0.05×0.03	0.31×0.21×0.05	0.14×0.13×0.09	0.13×0.09×0.02

SUPPORTING INFORMATION

T/K	123.00(10)	123.00(10)	123.00(10)	123.00(10)
Crystal System	orthorhombic	orthorhombic	orthorhombic	orthorhombic
Flack Parameter	-0.026(4)	-0.0208(19)	-0.021(4)	0.038(5)
Space Group	Fdd2	Fdd2	Fdd2	Fdd2
a/Å	42.9671(15)	42.9439(4)	42.8757(4)	43.0106(9)
b/Å	41.4521(15)	41.5068(5)	41.4125(4)	41.4566(11)
c/Å	11.7650(4)	11.7346(2)	11.74980(10)	11.7730(3)
a/°	90	90	90	90
b/°	90	90	90	90
g/°	90	90	90	90
V/Å ³	20954.3(13)	20916.5(5)	20862.8(3)	20992.1(9)
Z	8	8	8	8
Z'	0.5	0.5	0.5	0.5
Wavelength/Å	0.71073	0.71073	0.71073	0.71073
Radiation type	Mo Ka	Mo Ka	Mo Ka	Mo Ka
Q _{min} /°	2.182	2.136	2.297	2.6670
Q _{max} /°	26.372	26.372	26.372	31.3460
Measured Refl.	29395	145543	132317	51880
Independent Refl.	10423	10677	10662	10713
Reflections with I > 2(I)	9682	10473	10274	10226
R _{int}	0.0230	0.0299	0.0884	0.1340
Parameters	612	604	604	612
Restraints	1	1	1	1
Largest Peak	0.73	0.76	2.02	0.80
Deepest Hole	-0.59	-0.93	-1.57	-0.53
GooF	1.028	1.030	1.046	1.030
wR ₂ (all data) ^[a]	0.0634	0.0576	0.0946	0.0714
wR ₂	0.0618	0.0573	0.0934	0.0704
R ₁ (all data) ^[b]	0.0300	0.0227	0.0377	0.0317
R ₁	0.0259	0.0222	0.0364	0.0295

[a] $wR_2 = [\sum w (F_o^2 - F_c^2)^2 / \sum w (F_o^2)^2]^{1/2}$. [b] $R_1 = \sum ||F_o| - |F_c|| / \sum |F_o|$.

SUPPORTING INFORMATION

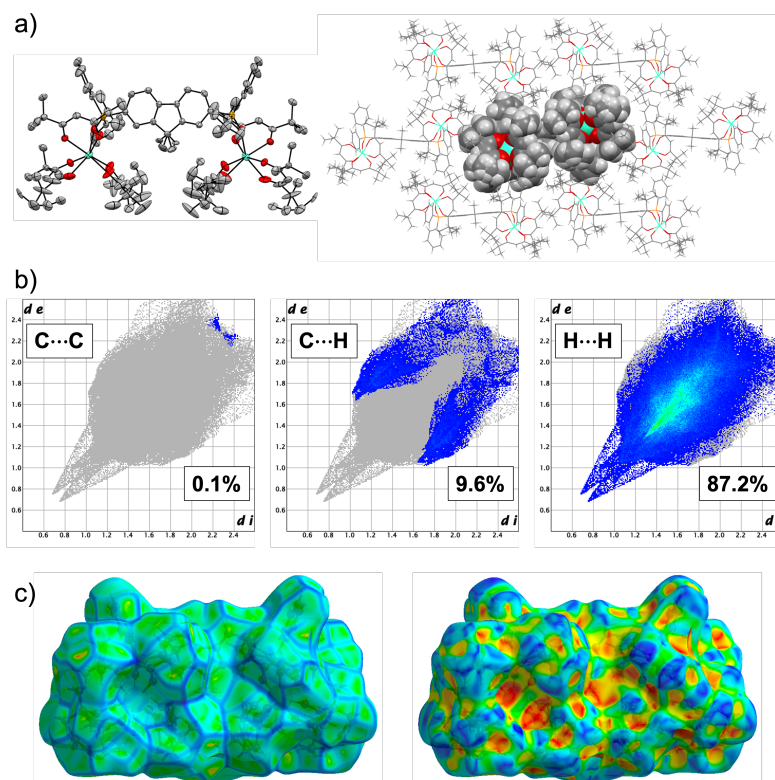


Figure S1. a) ORTEP view of a dinuclear unit (left, thermal ellipsoids are shown at 50% probability) and packing diagram (right), b) fingerprint plots for specific pairs of atom-types (grey shadow: outline of the complete fingerprint plot, d_i and d_e : distances from the Hirshfeld surfaces to the nearest nucleus inside and outside the surface, respectively), c) Hirshfeld surfaces with curvedness (left) and shape index (right) of $Tb_2(tmh)_6(dpbf)$.

Photophysical Measurements

PL emission and excitation spectra were recorded on a HORIBA Fluorolog-3 spectrofluorometer and corrected for the response of the detector system. The emission quantum yields were estimated using QuantaPhi Luminescence Yield System ($\varphi = 150$ mm). The wavelength dependence of the detector response and the beam intensity of Xe light source for each spectrum were calibrated using a standard light source. The TL/PL spectral measurements were performed on a CCD-based spectrograph QEPro from Ocean Optics (Figure S2 shows the experimental setup). Diffuse-reflectance spectra were recorded on a JASCO V-7200 UV-VIS-NIR Spectrophotometer using a JASCO PSH-005 powder sample cell ($\varphi = 8$ mm).

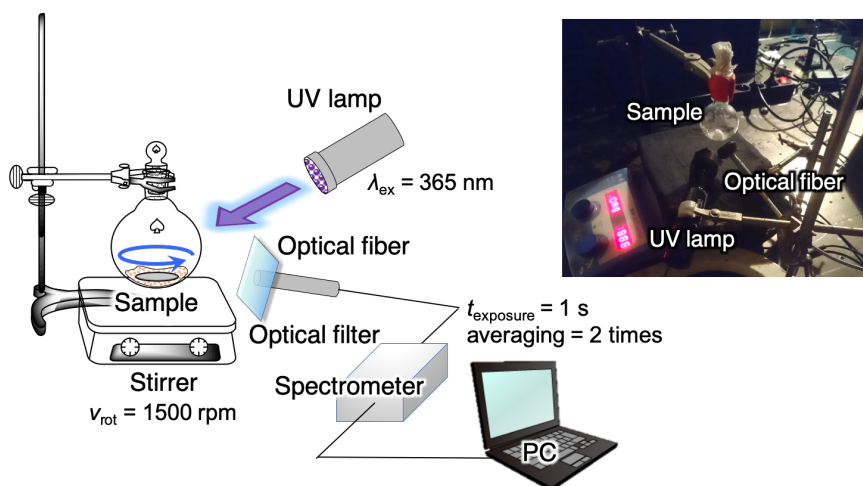


Figure S2. Experimental setups for TL/PL spectroscopy (UV lamp: $\lambda_{ex} = 365$ nm, Stirrer: $v_{rot} = 1500$ rpm, optical filter: 390 nm longpass, CCD camera: exposure time = 1000 ms, averaging = 2 times).

Nanomechanical tests

The target crystals were glued on a glass plate with a Crystalbond™ 509 mounting adhesive using a micromanipulator (Figure S3). Nanoindentations were carried out on a Triboindenter system (Hysitron Inc. Triboindenter T1950) equipped with a 60° 3-sided pyramidal

SUPPORTING INFORMATION

tip on fused quartz (Hysitron Inc. Ti-0038). All experiments were performed in the load-controlled mode using a loading/unloading time of 10 s and a hold time of 10 s at peak load (50–400 μN). More than 3 sets of 81 indentations (9×9 array) were performed on each crystal (Figure S3). Young's modulus and hardness were estimated from the unloading curves (see equations 2 and 3 below). In-situ SPM images were taken using the same probe after indentations.

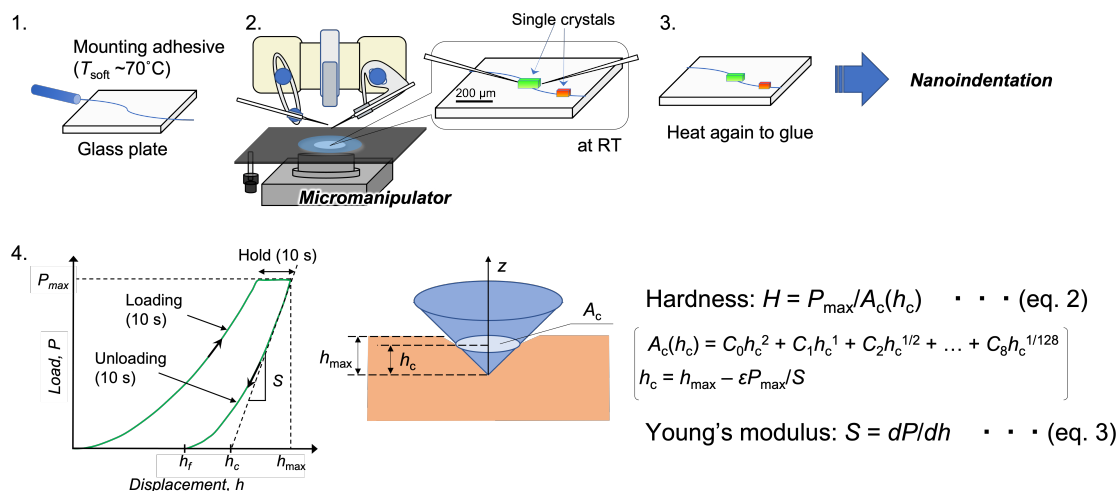


Figure S3. A sample preparation procedure for nanomechanical tests (A_c : area of contact, h_c : indent contact depth).

Synchrotron radiation wide-angle X-ray scattering (SR-WAXS) measurements

The measurements were performed using a BL-10C spectrometer at Photon Factory in High Energy Accelerator Research Organization (KEK, Tsukuba, Japan). The X-ray wavelength and the sample-to-detector distance were 1.55 Å and 24 cm, respectively. The X-ray scattering intensity was recorded by the PILATUS3 2M detector ($253.7 \times 288.8 \text{ cm}^2$ area, 172 μm pixel-resolution) from Dectris Co. The exposure time was 30 s. The powder samples were contained in sample cells with a pair of thin quartz windows, and their temperature was maintained at 25°C using a model mK2000 temperature controller (Instec, Inc., USA).

The background correction for the wide-angle scattering data was performed based on an ordinary method as follows;

$$I(q) = \frac{1}{B_{\text{sample}} T_{\text{sample}}} I_{\text{sample}}(q) - \frac{1}{B_{\text{cell}} T_{\text{cell}}} I_{\text{cell}}(q) \quad \text{--- (eq. 1),}$$

where $I_{\text{sample}}(q)$ and $I_{\text{cell}}(q)$ are the observed scattering intensities of the sample and the blank cell, respectively; B_{sample} and B_{cell} are the respective incident beam intensities; T_{sample} and T_{cell} are the respective transmissions. q is the scattering vector ($q = (4\pi/\lambda)\sin(\theta/2)$; θ : scattering angle; λ : X-ray wavelength).

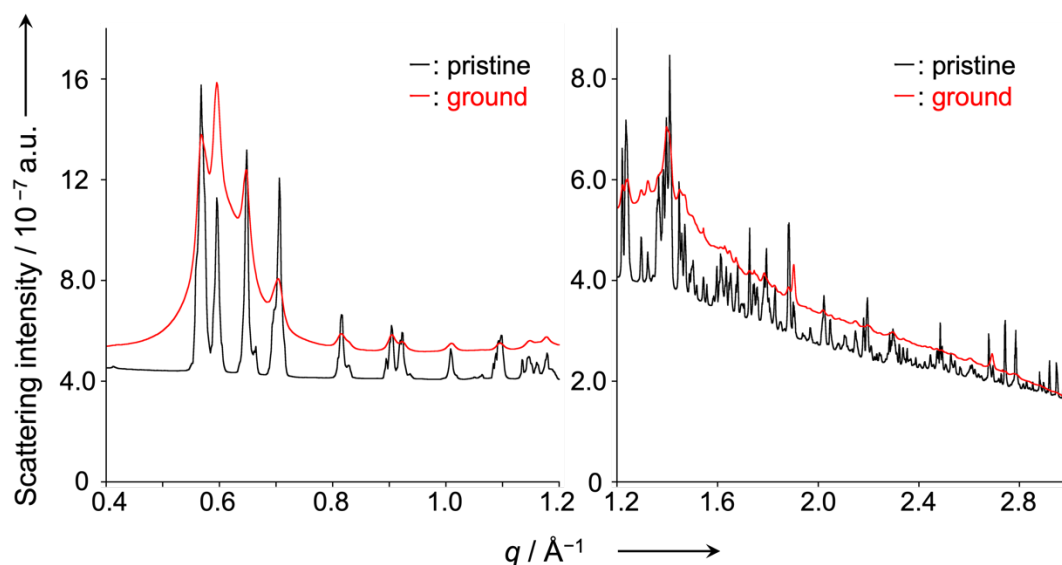


Figure S4. Synchrotron radiation wide-angle X-ray scattering (SR-WAXS) patterns of $[\text{Ln}_2(\text{tmh})_6(\text{dpdpf})]$ ($\text{Ln} = \text{Tb}$) in pristine (black lines) and in ground (red lines) forms.

SUPPORTING INFORMATION

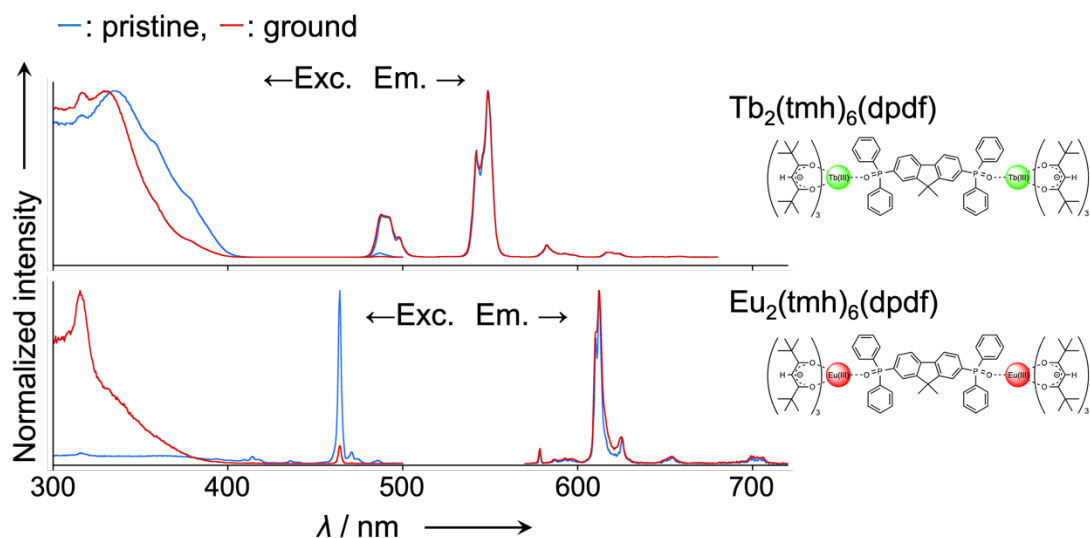


Figure S5. PL excitation/emission spectra ($\lambda_{\text{exc}} = 340$ nm, $\lambda_{\text{obs, Eu}} = 613$ nm, $\lambda_{\text{obs, Tb}} = 545$ nm) of $\text{Eu}_2(\text{tmh})_6(\text{dpdpf})$ and $\text{Tb}_2(\text{tmh})_6(\text{dpdpf})$ in pristine (blue lines) and in ground (red lines) forms.

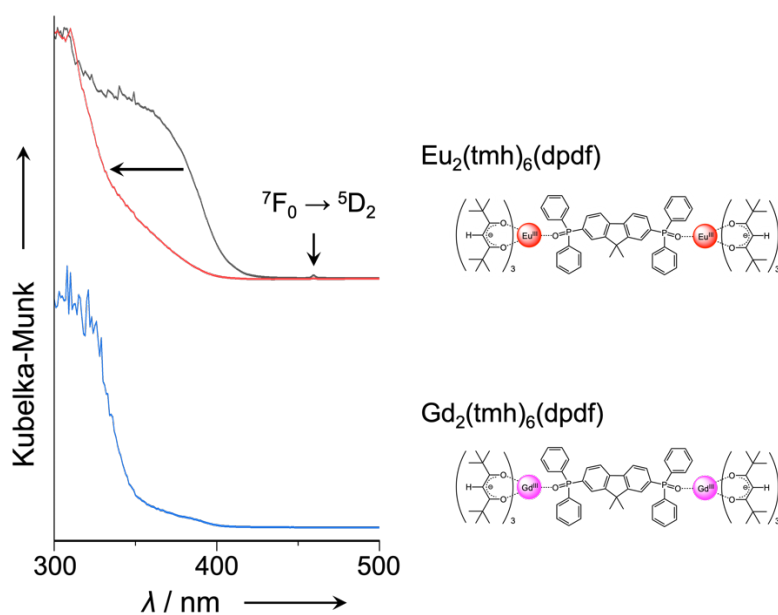


Figure S6. Diffuse-reflectance spectra of $\text{Eu}_2(\text{tmh})_6(\text{dpdpf})$ (black: pristine, red: ground) and $\text{Gd}_2(\text{tmh})_6(\text{dpdpf})$ (blue: pristine) in solid state.

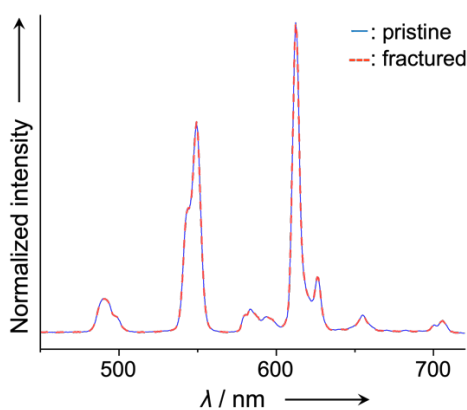


Figure S7. PL spectra of $\text{EuTb}(\text{tmh})_6(\text{dpdpf})$ before and after fracturing (blue solid and red dotted lines, respectively, $\lambda_{\text{ex}} = 365$ nm).

SUPPORTING INFORMATION

Table S2. Spectral intensity ratio ($I_{\text{Eu}}/I_{\text{Tb}}$) of $\text{EuTb}(\text{tmh})_3(\text{dpdf})$ before/during/after fracturing.

	Before fracturing	During fracturing									After fracturing	
	PL1	TL1	TL2	TL3	TL4	TL5	TL6	TL7	TL8	TL9	TL10	PL2
$I_{\text{Eu}}/I_{\text{Tb}}$	1.48	0.98	1.00	1.01	1.05	1.09	1.04	0.86	1.01	0.96	1.05	1.47
Ave.	-					1.00						-
Stdev.	-					0.06						-

Each measurement was averaged by two sets of 1 s exposure.

Photography

TL pictures in Figure 2 and Figure 4a bottom in main text were trimmed from a video recorded on an Olympus pen e-pl5 with a M. ZUIKO DIGITAL 17 mm F1.8 lens. The close-up PL pictures of the solid samples before/after grinding (Figure 4a top in main text) under white LED/UV were taken using a digital optical microscope (Keyence VHX-5000) equipped with objectives VH-Z20R/W/T.

Reference

[28] K. Yanagisawa, T. Nakanishi, Y. Kitagawa, T. Seki, T. Akama, M. Kobayashi, H. Ito, K. Fushimi, Y. Hasegawa, *Eur. J. Inorg. Chem.* **2015**, 28, 4769-4774.

Author Contributions

Y. H.* designed the research and prepared the manuscript. S. V.-D. performed the spectroscopy and photography. T. O. analyzed the results of nanoindentation experiments. Y. K. and Y. H. assisted the molecular design and synthesis. T. N. and T. T. analyzed the crystallographic information. R. M. and C. A. helped the instrumentation for the TL/PL/MCL spectroscopy. All authors joined the discussions and thoroughly checked the manuscript.